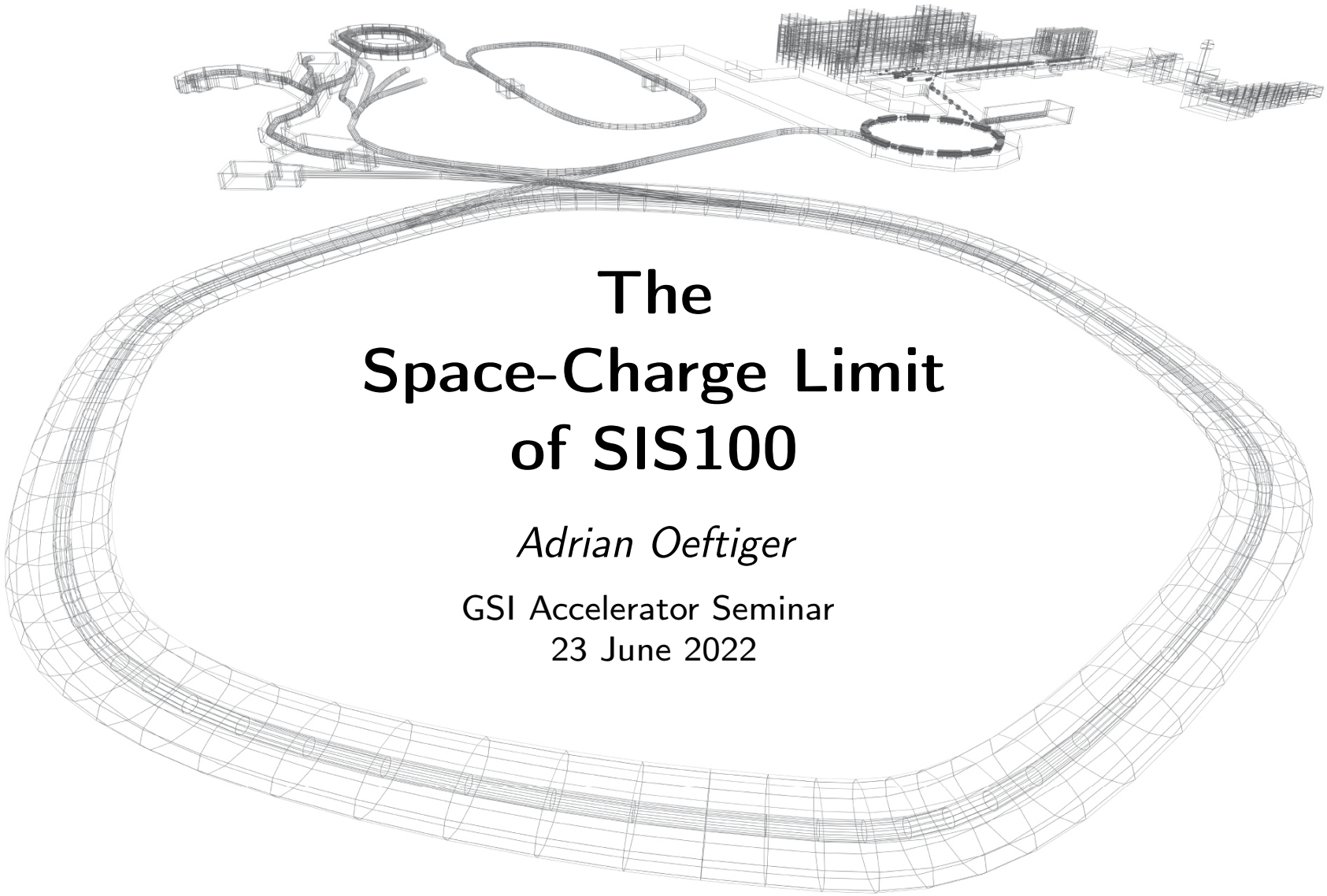

The Space-Charge Limit of SIS100

Adrian Oeftiger

GSI Accelerator Seminar
23 June 2022

Abstract

As the key synchrotron of FAIR, SIS100 should be operated at the "space charge limit" for light- and heavy-ion beams. While delivering maximum intensities, the beam losses due to space-charge-induced resonance crossing should not exceed a few percent during a full cycle. The one-second-long injection plateau poses the most critical challenge in terms of beam dynamics – in particular for the U^{28+} beams. Based on the recent progress on cold bench measurements of the SIS100 dipole and quadrupole magnets, as well as the newly established GPU-accelerated SIS100 tracking simulation suite, we are now in position to realistically model and explore the space charge limit of SIS100.

This talk presents the recently published extensive results on SIS100 performance at the space charge limit. We discuss the magnet field error model and the correspondingly driven betatron resonances. A key aspect is the comparison of 3D space charge models, validating the fast approximative solver results with fully self-consistent computations, for the first time for long-term conditions. We identify the achievable maximum beam intensity from simulations covering the full duration of the injection plateau. We conclude with discussing several countermeasures to increase the space charge limit: beta-beat compensation, double-harmonic rf bunch flattening, and finally the promising novel technique of space charge compensation with electron lenses.

Motivation

Overview:

- SIS100: deliver high-intensity beams

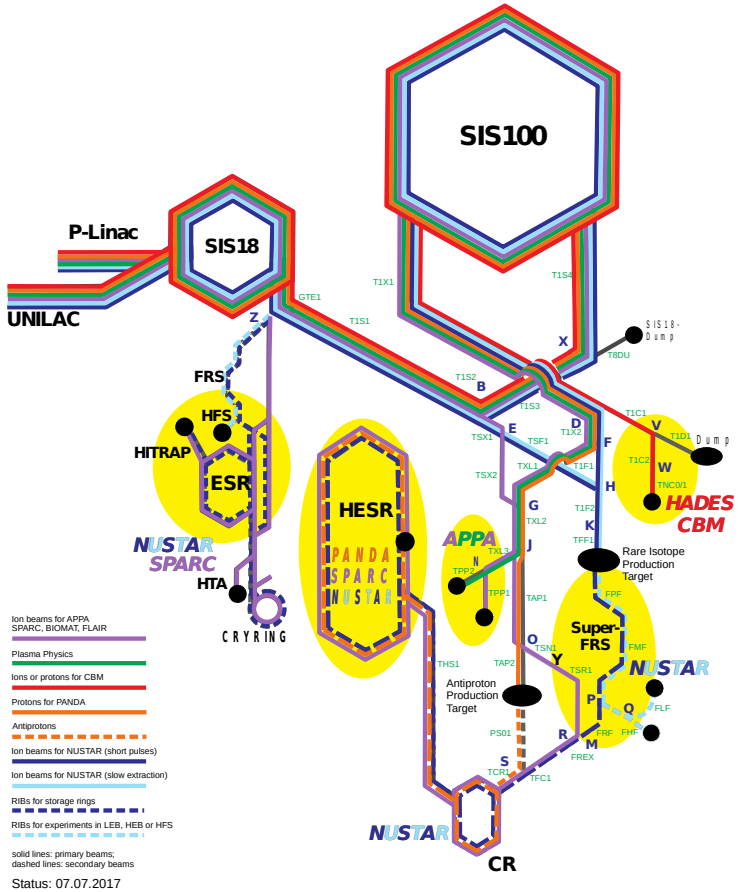

Figure: FAIR complex

Motivation

Overview:

- SIS100: deliver high-intensity beams
- crucial for performance: maintain beam quality during 1-sec injection plateau
- uranium U^{28+} beam most critical:
  - largest beam size vs. transverse aperture
  - space-charge induced losses
    $\rightsquigarrow$ dynamic vacuum issues

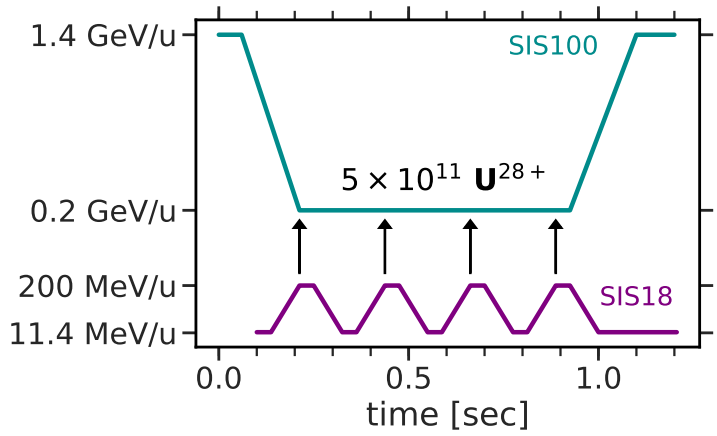

Figure: SIS18 to SIS100 transfer

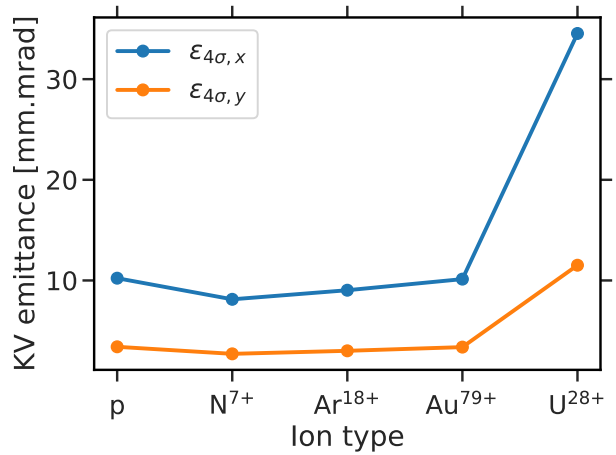

Figure: scaled beam sizes at 18 T m

Motivation

Overview:

- SIS100: deliver high-intensity beams
- crucial for performance: maintain beam quality during 1-sec injection plateau
- uranium U^{28+} beam most critical:
  - largest beam size vs. transverse aperture
  - space-charge induced losses
    $\rightsquigarrow$ dynamic vacuum issues
- challenge: efficient numerical model for injection plateau

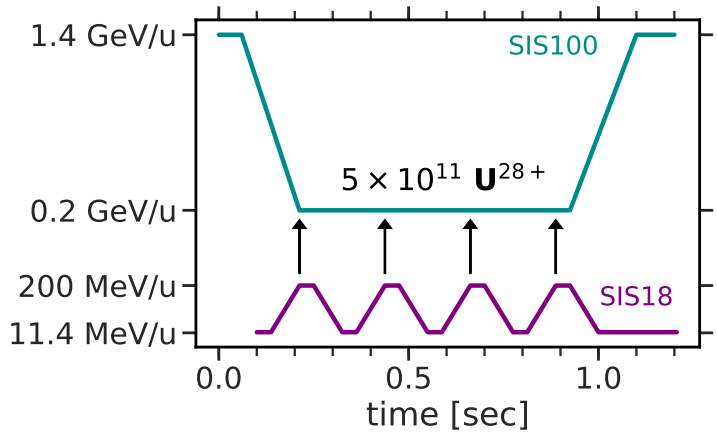

Figure: SIS18 to SIS100 transfer

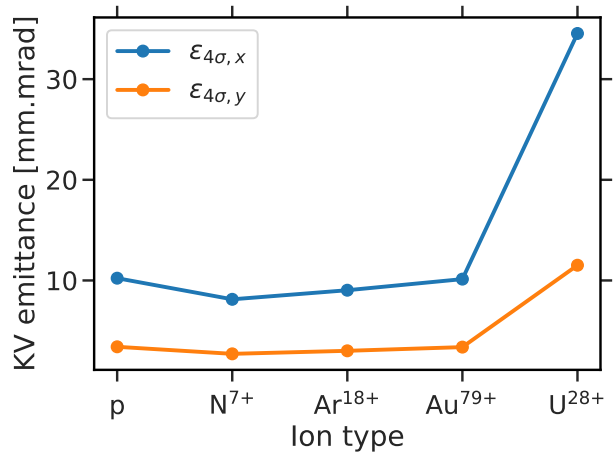

Figure: scaled beam sizes at 18 T m

Contents

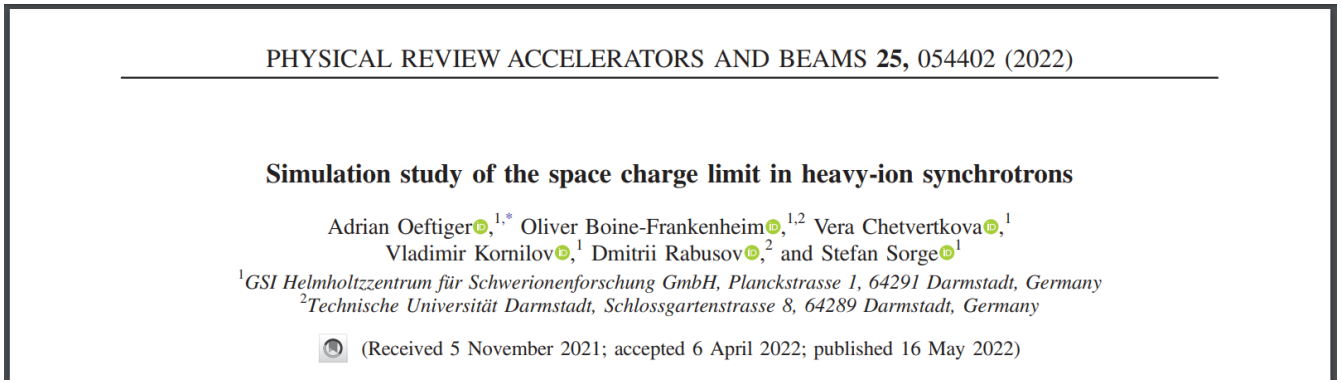

PHYSICAL REVIEW ACCELERATORS AND BEAMS **25,** 054402 (2022)

Simulation study of the space charge limit in heavy-ion synchrotrons

Adrian Oeftiger,[1,*] Oliver Boine-Frankenheim,[1,2] Vera Chetvertkova,[1]
Vladimir Kornilov,[1] Dmitrii Rabusov,[2] and Stefan Sorge[1]

[1]*GSI Helmholtzzentrum für Schwerionenforschung GmbH, Planckstrasse 1, 64291 Darmstadt, Germany*
[2]*Technische Universität Darmstadt, Schlossgartenstrasse 8, 64289 Darmstadt, Germany*

(Received 5 November 2021; accepted 6 April 2022; published 16 May 2022)

Key ingredients of study:

1. detailed model for **magnetic field errors** from cold bench measurements
2. **full tracking model** of machine lattice
3. detailed **space charge** models
   - self-consistent 3D PIC solver (particle-in-cell)
   - fast (approximative) frozen field maps

   $\Longrightarrow$ parallelised on multi-core CPU and GPU architectures

Contents

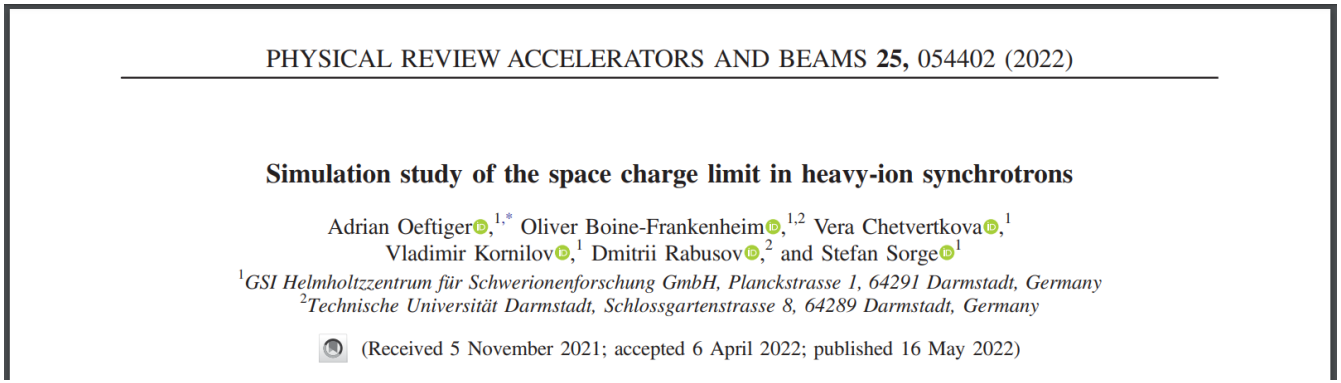

PHYSICAL REVIEW ACCELERATORS AND BEAMS **25,** 054402 (2022)

Simulation study of the space charge limit in heavy-ion synchrotrons

Adrian Oeftiger,[1,*] Oliver Boine-Frankenheim,[1,2] Vera Chetvertkova,[1]
Vladimir Kornilov,[1] Dmitrii Rabusov,[2] and Stefan Sorge[1]

[1]*GSI Helmholtzzentrum für Schwerionenforschung GmbH, Planckstrasse 1, 64291 Darmstadt, Germany*
[2]*Technische Universität Darmstadt, Schlossgartenstrasse 8, 64289 Darmstadt, Germany*

(Received 5 November 2021; accepted 6 April 2022; published 16 May 2022)

Structure:

A. The Model
B. Betatron Resonances:
   - Intrinsic from Space Charge
   - External from Field Errors
C. Space-Charge Limit
D. Mitigation Measures

A. The Model

Space Charge Modelling

Simulation model:

- track macro-particles (m.p.) through accelerator lattice & space charge kicks

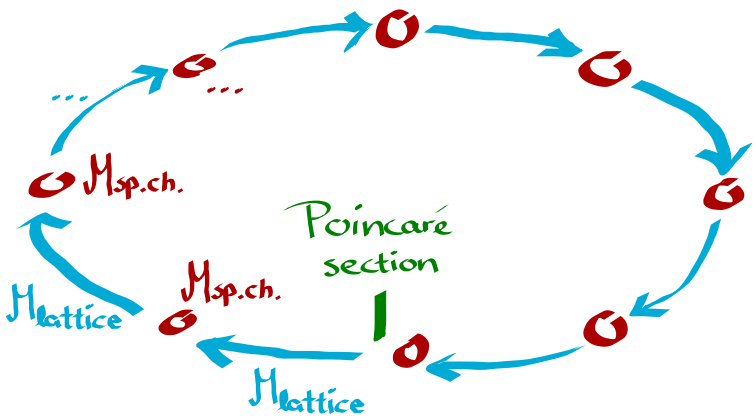

Figure: sketch of simulation model

Space Charge Modelling

Simulation model:

- track macro-particles (m.p.) through accelerator lattice & space charge kicks
- nonlinear 3D space charge (SC) models:
  - *self-consistent:* PIC solves Poisson equation for m.p. distribution
  - *fixed frozen:* constant field map independent of m.p. dynamics
  - (*adaptive frozen:* frozen field map scaled with m.p. distribution momenta)

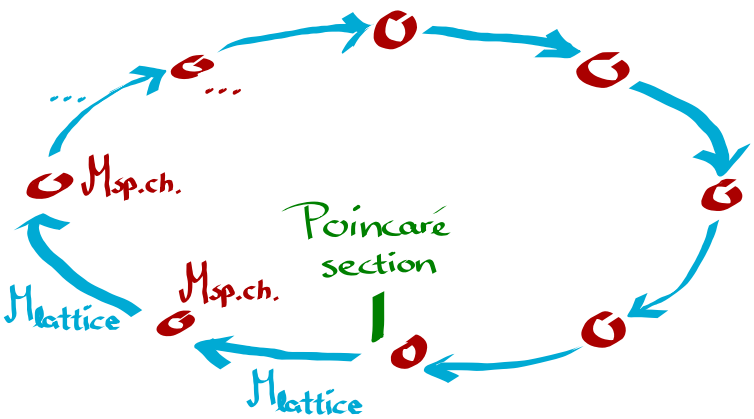

Figure: sketch of simulation model

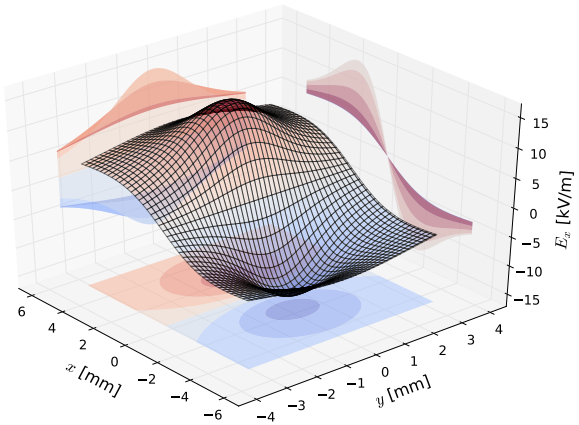

Figure: horizontal space charge field

Space Charge Modelling

Simulation model:

- track macro-particles (m.p.) through accelerator lattice & space charge kicks
- nonlinear 3D space charge (SC) models:
  - *self-consistent:* PIC solves Poisson equation for m.p. distribution
  - *fixed frozen:* constant field map independent of m.p. dynamics

Maximum SC Tune Shift

$$\Delta Q_y^{\mathrm{SC}} = -\frac{Ze}{4\pi\epsilon_0 m_0 c^2} \frac{\lambda_{\max}}{\beta^2\gamma^3} \frac{1}{2\pi} \oint ds \frac{\beta_y(s)}{\sigma_y(s)(\sigma_x(s)+\sigma_y(s))}$$

Figure: sketch of simulation model

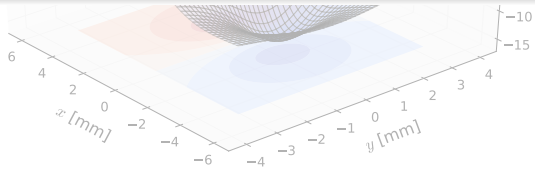

Figure: horizontal space charge field

Beam Parameters

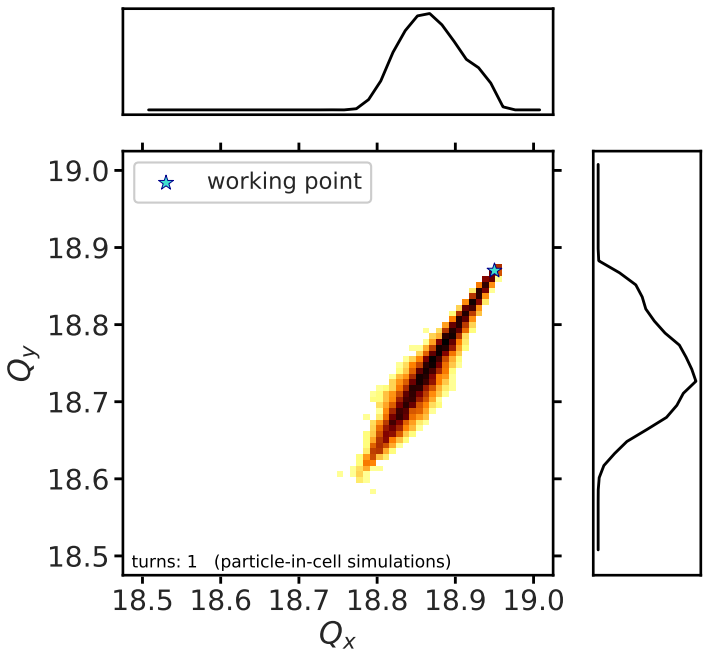

Figure: space charge tune footprint

Table: Considered Parameters for $^{238}U^{28+}$ Accumulation at SIS100 Injection Energy

Parameter	Value
Hor. norm. rms emittance ϵ_x	5.9 mm mrad
Vert. norm. rms emittance ϵ_y	2.5 mm mrad
Rms bunch length σ_z	13.2 m
Bunch intensity N of U_{238}^{28+} ions	0.625×10^{11}
Max. space charge ΔQ_y^{SC}	−0.30
Rms chromatic $Q'_{x,y} \cdot \sigma_{\Delta p/p_0}$	0.01
Synchrotron tune Q_s	4.5×10^{-3}
Kinetic energy	$E_{kin} = 200\,\mathrm{MeV/u}$
Relativistic β factor	0.568
Revolution frequency f_{rev}	157 kHz

B. Betatron Resonances

Only Space Charge

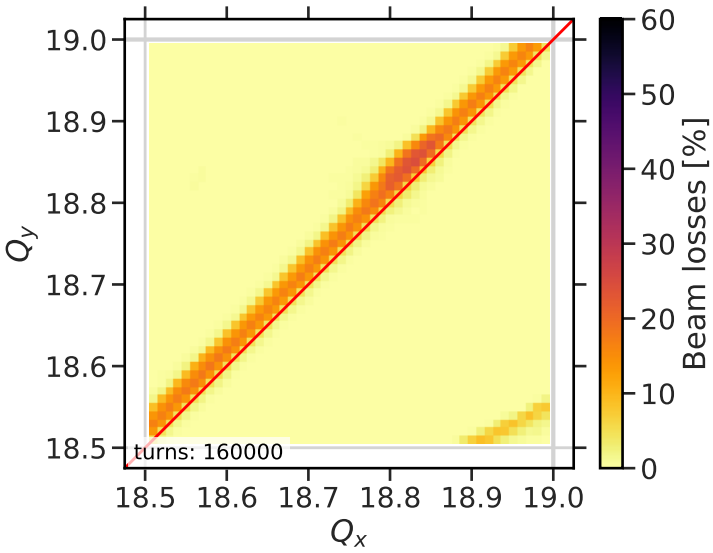

Figure: tune diagram of beam loss

Cold, error-free, symmetric SIS100 lattice:

- perfect dipole and quadrupole magnets
- symmetry of $S = 6$ maintained (no warm / normalconducting quadrupoles)
- space charge → only source for resonances
- simulated for 160'000 turns = 1 second

$\Longrightarrow$ mainly Montague resonance visible

$\Longrightarrow$ absence of low-order structure resonances!

Only Space Charge

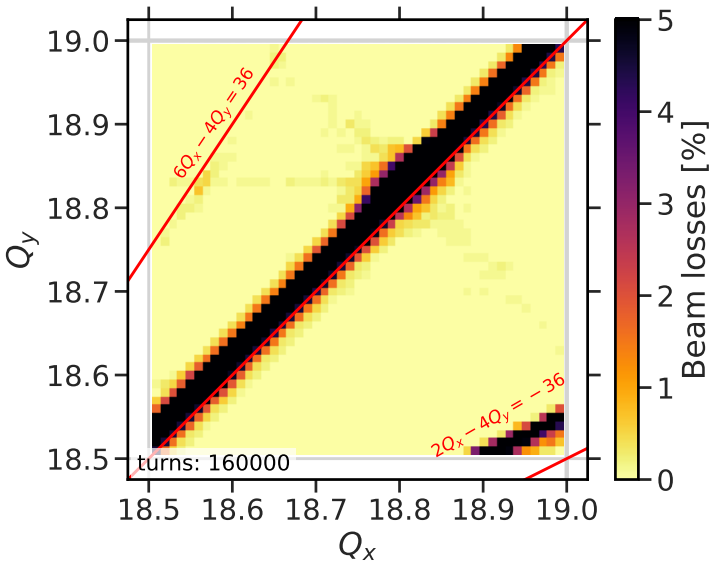

Figure: tune diagram of beam loss

Cold, error-free, symmetric SIS100 lattice:

- perfect dipole and quadrupole magnets
- symmetry of $S = 6$ maintained (no warm / normalconducting quadrupoles)
- space charge → only source for resonances
- simulated for 160'000 turns = 1 second

$\Longrightarrow$ mainly Montague resonance visible

$\Longrightarrow$ absence of low-order structure resonances!

Montague Resonance

Montague resonance $2Q_x - 2Q_y = 0$:

- 4^{th}-order resonance
- intrinsically driven by space charge
- transverse emittance exchange for anisotropic beams

$\Longrightarrow$ stopband always present around $Q_x \approx Q_y$ for SIS100 beams

Space charge model predictions:

– "adaptive frozen" resolves full exchange but predicts too large stopband extent

\+ "fixed frozen" resolves stopband edges well!

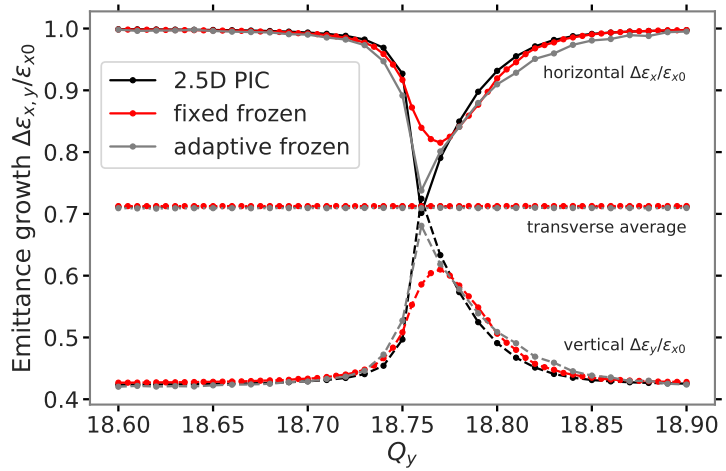

Figure: emittance exchange

Montague Resonance

Montague resonance $2Q_x - 2Q_y = 0$:

- 4^{th}-order resonance
- intrinsically driven by space charge
- transverse emittance exchange for anis
- $\Longrightarrow$ stop for

Observation

"Fixed frozen" model better suited than "adaptive frozen" to approximate realistic PIC when identifying loss-free conditions!

Space charge model predictions:

- – "adaptive frozen" resolves full exchange but predicts too large stopband extent
- \+ "fixed frozen" resolves stopband edges well!

Figure: emittance exchange

Warm Quadrupoles

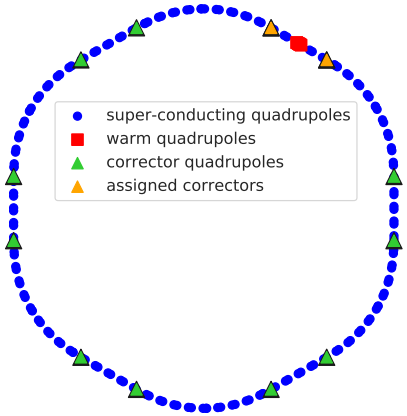

Figure: SIS100 quadrupole survey [courtesy D. Rabusov]

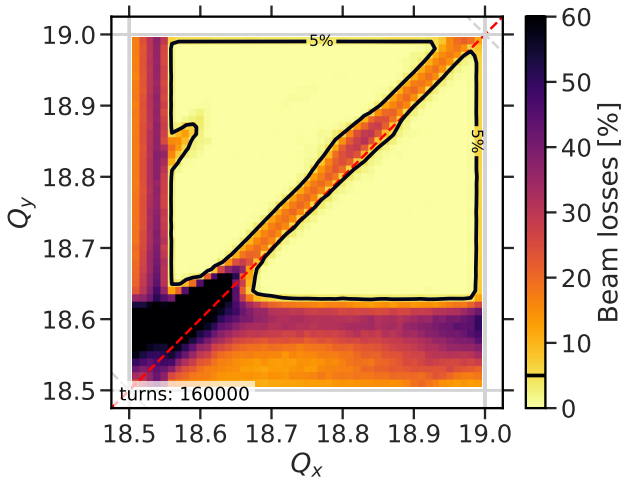

Figure: corrected warm quadrupoles

Real SIS100 lattice:

- 2 cold quadrupoles replaced by warm / normalconducting quadrupoles (radiation hardened, required in extraction region)
- breaking of $S = 6$ symmetry

$\Longrightarrow$ gradient error

$\Longrightarrow$ externally driven half-integer resonance

Warm Quadrupoles

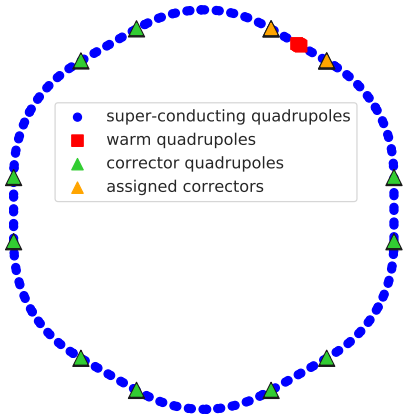

Figure: SIS100 quadrupole survey [courtesy D. Rabusov]

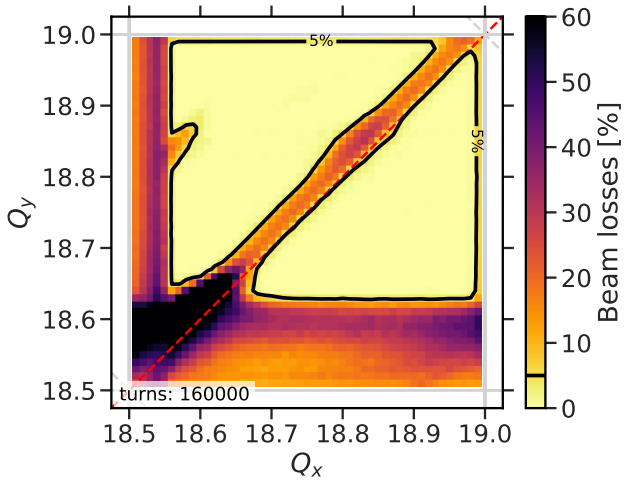

Figure: corrected warm quadrupoles

Real SIS100 lattice:

- 2 cold quadrupoles replaced by warm / normalconducting quadrupoles (radiation hardened, required in extraction region)
- breaking of $S = 6$ symmetry

$\Longrightarrow$ gradient error

$\Longrightarrow$ externally driven half-integer resonance

$\Longrightarrow$ can be minimised by quadrupole correctors

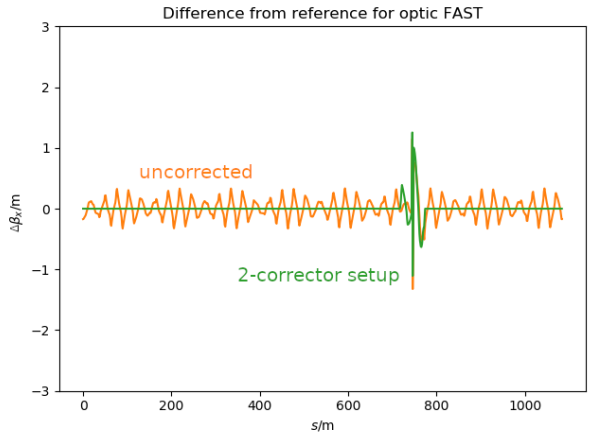

Figure: β-beat around SIS100 [courtesy D. Ondreka]

Half-integer Resonance

Half-integer stopband:

- without space charge, without $\Delta p/p_0$: $\delta Q_{\text{stopband}} = 0.023$
- without space charge, with $\Delta p/p_0$: $\delta Q_{\text{stopband}} \sim 0.1$
- with space charge: $\delta Q_{\text{stopband}} \sim 0.25$

$\Longrightarrow$ fixed frozen SC model reproduces stopband edges from PIC

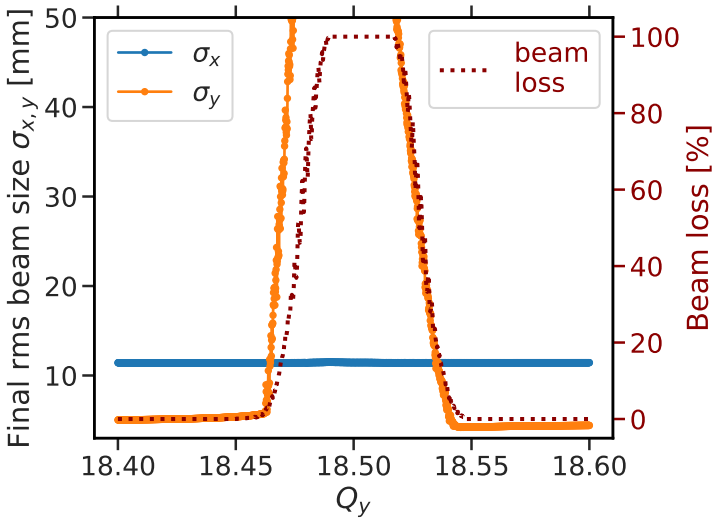

Figure: no space charge

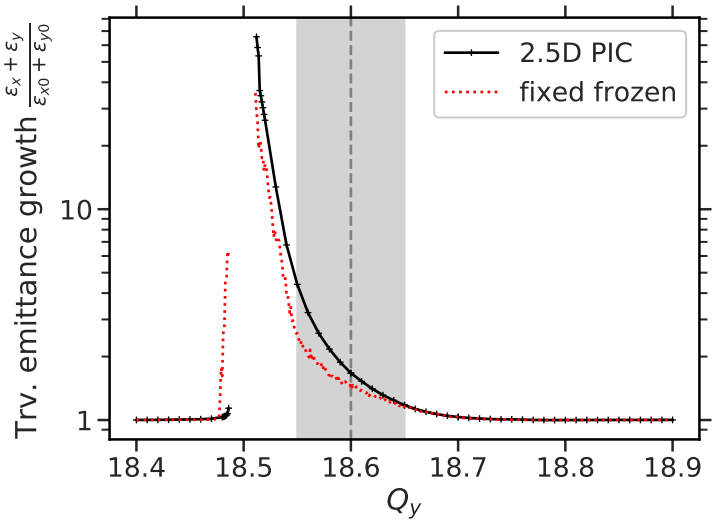

Figure: with space charge

Field Error Model

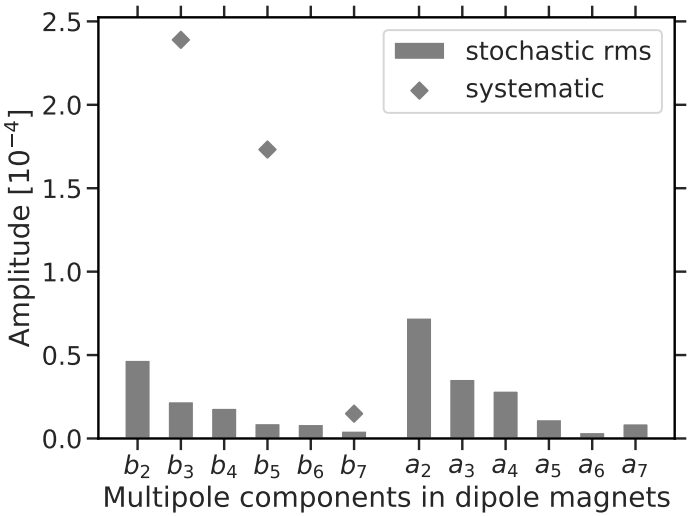

Figure: dipole magnets

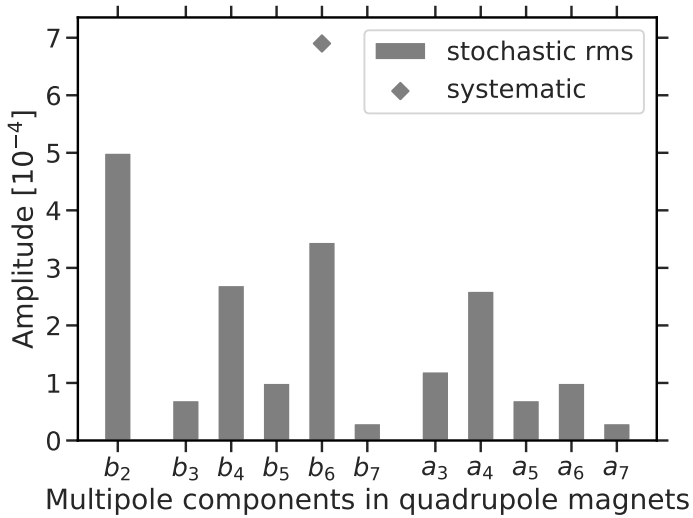

Figure: quadrupole magnets

Field error model extracted from cold bench measurements of magnet units:

- stochastic amplitudes drive non-systematic resonances
- random number sequence → multipole errors for every dipole and quadrupole magnet

quadrupole model displayed here corresponds to PRAB paper version (based on stamped FoS), see GSI-2021-00450 report ↗ for model based on series production and its comparison

Full Model with Space Charge

Linear and nonlinear resonances driven by magnet field errors. Resonance condition without space charge:

$$mQ_x + nQ_y = p \qquad \text{for} \quad m, n, p \in \mathbb{Z}$$

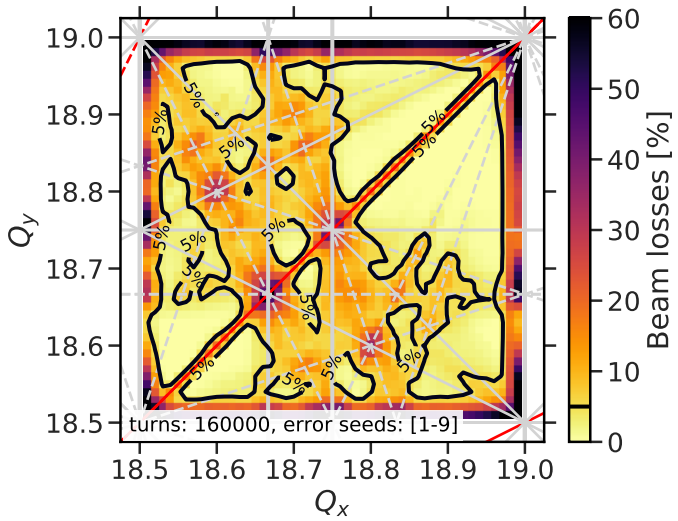

Figure: no space charge

Full Model with Space Charge

Linear and nonlinear resonances driven by magnet field errors. Resonance condition without space charge:

$$mQ_x + nQ_y = p \qquad \text{for} \quad m, n, p \in \mathbb{Z}$$

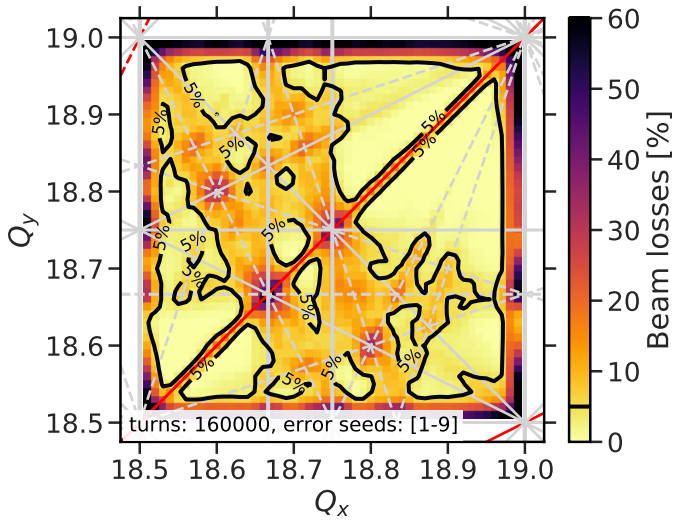

Figure: no space charge

include
$\Longrightarrow$
SC

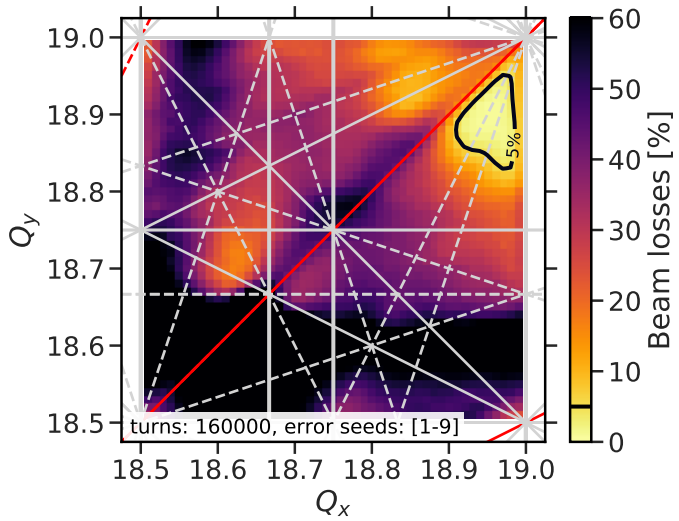

Figure: with fixed frozen space charge

$\longrightarrow$ SC broadens existing resonance stopbands

$\Longrightarrow$ optimal working point area around $(Q_x, Q_y) = (18.95, 18.87)$
[requires transverse feedback system to fight resistive wall instability!]

Validation with Self-consistent PIC

Self-consistent PIC simulations:

- have already validated isolated (1) space-charge-driven (Montague) and (2) gradient-error-driven stopband predictions from fixed frozen SC (FFSC)

→ now validate full error model FFSC predictions for beam loss

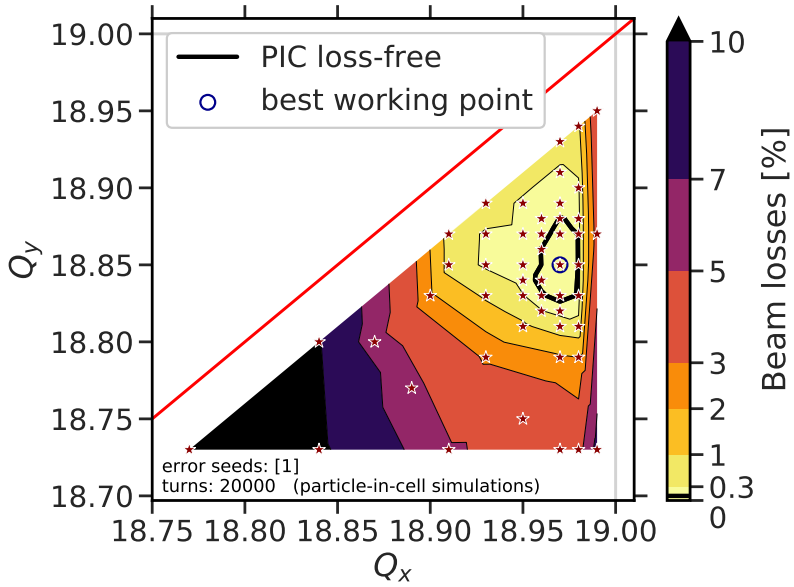

Figure: self-consistent PIC simulations

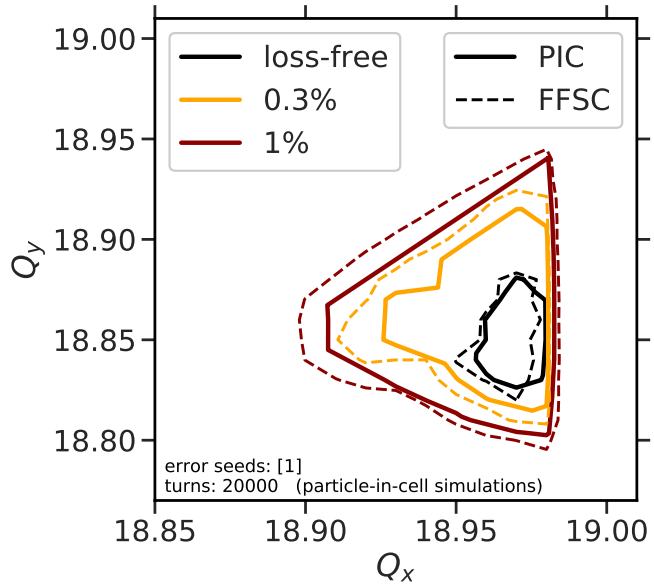

Figure: comparison between SC models

note: PIC simulations take 2 days (on NVIDIA V100 GPU) vs. FFSC simulations with 7 min (on 16 CPU cores, HPC AMD)

Relevant Field Error Orders

Major resonances confining low-loss area:

- top left: Montague resonance
- right: integer resonance $Q_x = 19$
- bottom: higher-order resonances

Simulations with reduced field error model:

- identify sextupole and octupole orders $n = 3, 4$ as main limitation towards low Q_y

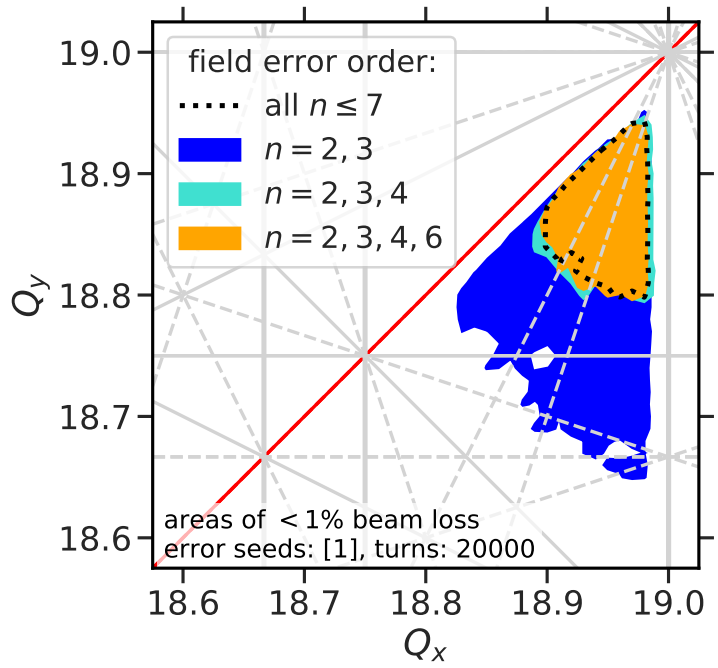

Figure: low-loss tune areas vs. multipole order

C. Space-Charge Limit

Space-Charge Limit

Keeping all beam parameters identical, increasing N:

⟶ **dynamic definition of space-charge limit**: reached when loss-free working point area vanishes

⟹ U^{28+} space-charge limit at **120%** of nominal bunch intensity N_0

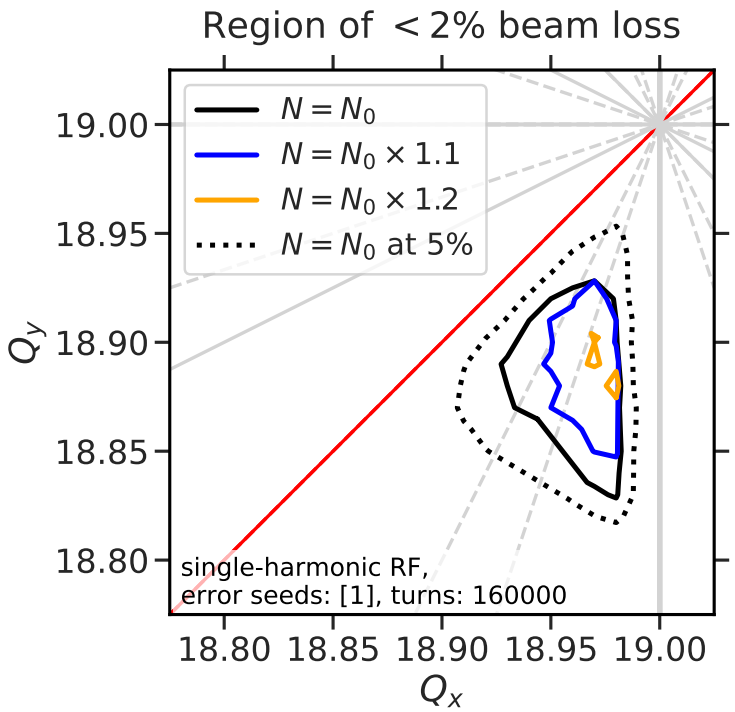

Figure: low-loss area for increasing N

D. Mitigation Measures

Correction of β-beat

Two sources of β-beat (gradient error):

- warm quadrupoles: uncorrected = 2%
  - $\longrightarrow$ significant effect on low-loss area size
  - $\Longrightarrow$ important to control

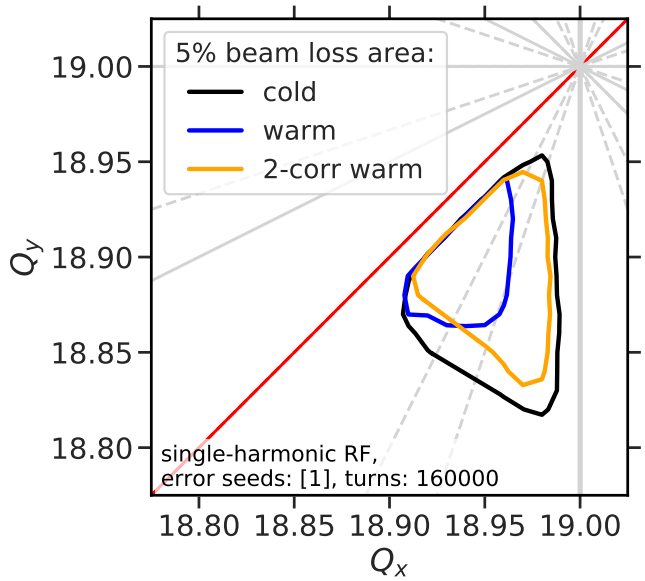

Figure: low-loss area with warm quadrupoles

Correction of β-beat

Two sources of β-beat (gradient error):

- warm quadrupoles: uncorrected = 2%
  - $\longrightarrow$ significant effect on low-loss area size
  - $\Longrightarrow$ important to control
- distributed b_2: $\approx 0.5\%$
  (according to field error model)
  - $\Longrightarrow$ below $b_2 = 10$ units: no significant effect on low-loss area size

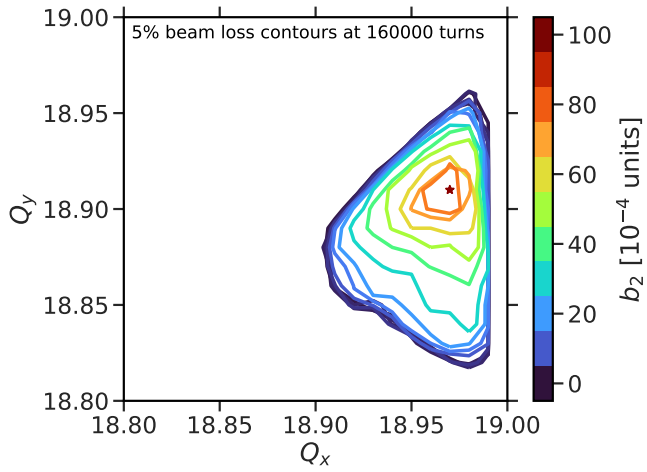

Figure: low-loss area with b_2

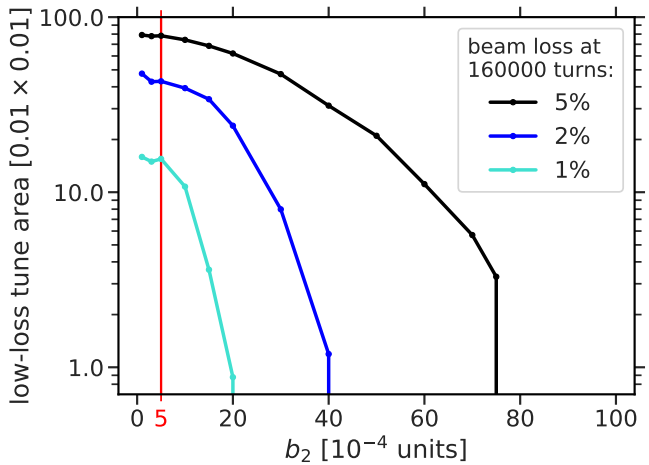

Figure: size of low-loss area vs. b_2

Double-harmonic RF

By adding $h = 20$ harmonic at half base RF voltage in bunch lengthening mode,

$$V_{h=20} = V_{h=10}/2$$

obtain flattened bunches with reduced line charge density at 80% of nominal $\lambda_{\max}$.

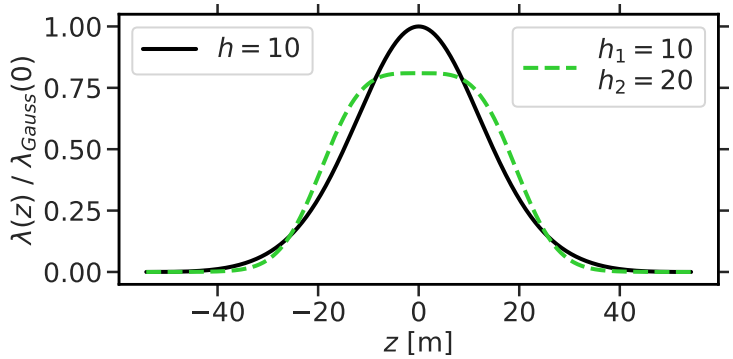

Figure: line densities

Results with Double-harmonic RF

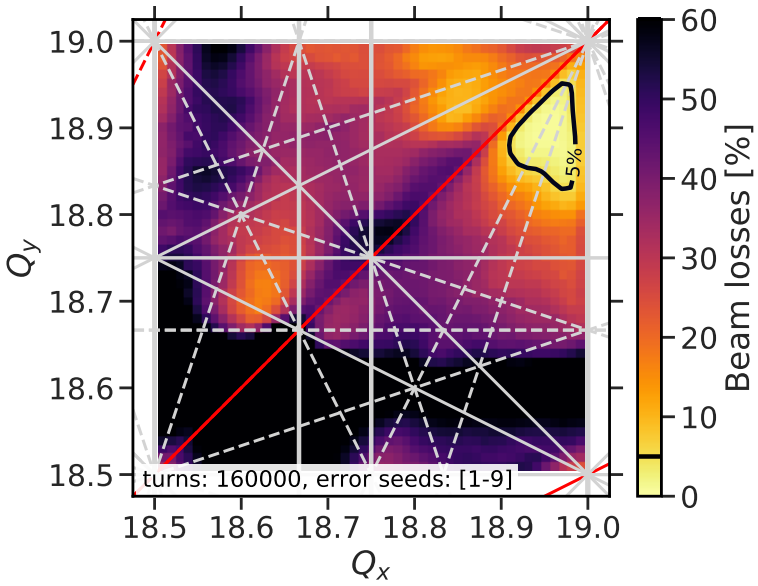

Figure: single-harmonic RF

flatten
$\Longrightarrow$
bunch

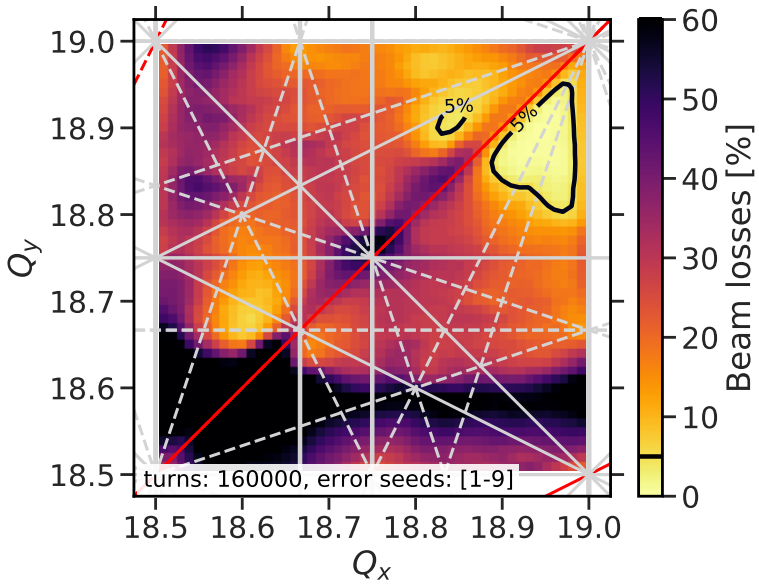

Figure: double-harmonic RF

Observations:

- black half-integer stopband shrinks by $\approx 20\%$
- low-loss area opens up

SC Limit with Double-harmonic RF

Increasing N for double-harmonic RF:

- find space-charge limit at **150%** of nominal intensity N_0

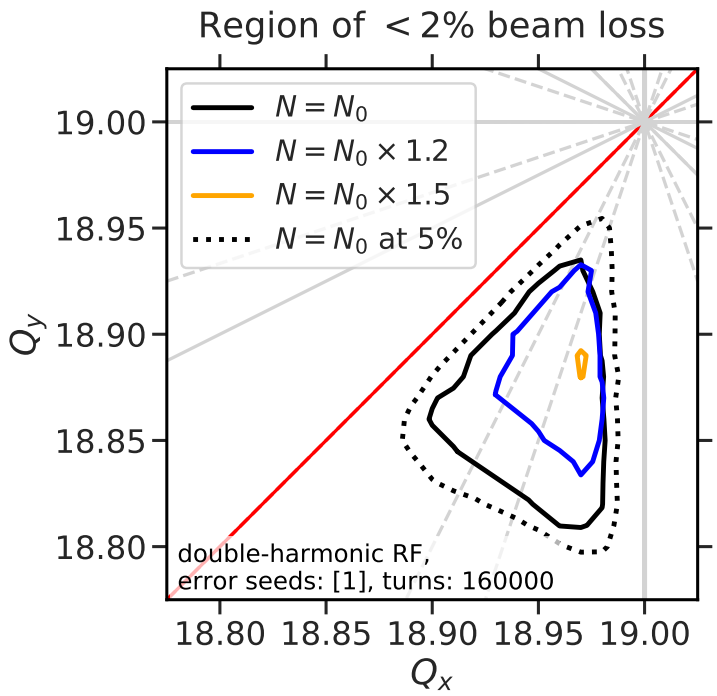

Figure: low-loss area for increasing N

Pulsed Electron Lenses

Pulsed electron lenses:

- short insertion with co-propagating electron beam
- transversely homogeneous distribution
- longitudinally modulated to match ion bunch profile

$\longrightarrow$ compensate longitudinal dependency of space charge
(ideal: half compensation of linear space charge tune shift, $\Delta Q_{\mathrm{elens}} = \Delta Q_{\mathrm{KV}}/2$)

$\Longrightarrow$ installing 3 such electron lenses shrinks stopbands!

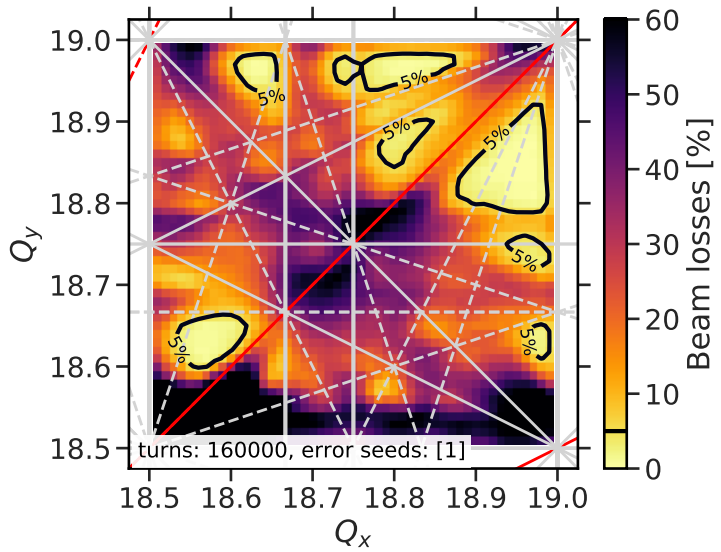

Figure: tune diagram at nominal N

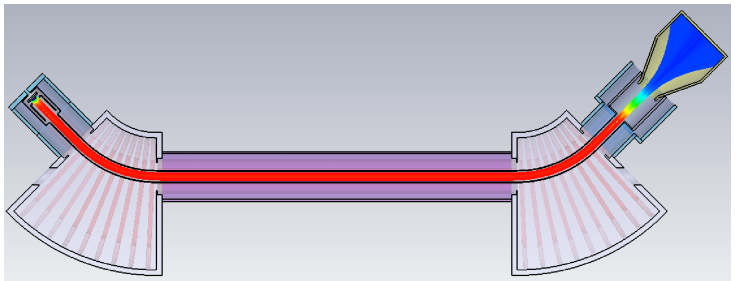

Figure: e-lens model for SIS18

Pulsed Electron Lenses

Pulsed electron lenses:

- short insertion with co-propagating electron beam
- transversely homogeneous distribution
- longitudinally modulated to match ion bunch profile

$\longrightarrow$ compensate longitudinal dependency of space charge
(ideal: half compensation of linear space charge tune shift, $\Delta Q_{\mathrm{elens}} = \Delta Q_{\mathrm{KV}}/2$)

$\Longrightarrow$ installing 3 such electron lenses shrinks stopbands!

$\Longrightarrow$ space-charge limit increased significantly!

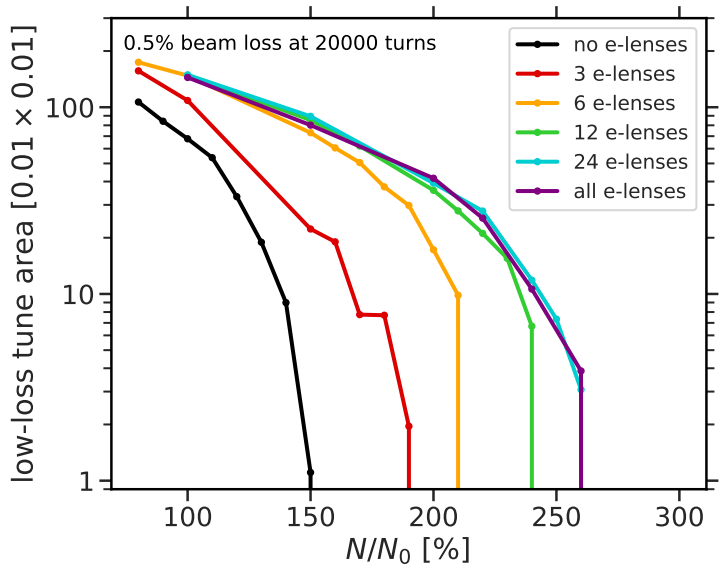

Figure: low-loss area for increasing N [preliminary, unpublished results]

Conclusion

Summary:

- validated fixed frozen SC model predictions by long-term PIC simulations
- identified **optimal tune area** around $(Q_x, Q_y) = (18.95, 18.87)$ for nominal SIS100 operation under strong space charge conditions
  - $\longrightarrow$ rigid constraints: Montague resonance (top left), integer resonance (right)
  - $\longrightarrow$ soft constraint: higher-order resonances (bottom)
- explored space-charge limit:
  - nominal SIS100: +20% intensity
  - double-harmonic RF: +50% intensity
  - 3 pulsed electron lenses: +80..90% intensity

Conclusion

Summary:

- validated fixed frozen SC model predictions by long-term PIC simulations
- identified **optimal tune area** around $(Q_x, Q_y) = (18.95, 18.87)$ for nominal SIS100 operation under strong space charge conditions
  - $\longrightarrow$ rigid constraints: Montague resonance (top left), integer resonance (right)
  - $\longrightarrow$ soft constraint: higher-order resonances (bottom)
- explored space-charge limit:
  - nominal SIS100: +20% intensity
  - double-harmonic RF: +50% intensity
  - 3 pulsed electron lenses: +80..90% intensity

Take-home message:

- fast and reliable simulation tool & model established
  - $\Longrightarrow$ identify low-loss accelerator settings
- nominal FAIR intensity $\rightarrow$ feasibility confirmed

... the new GPU cluster ...

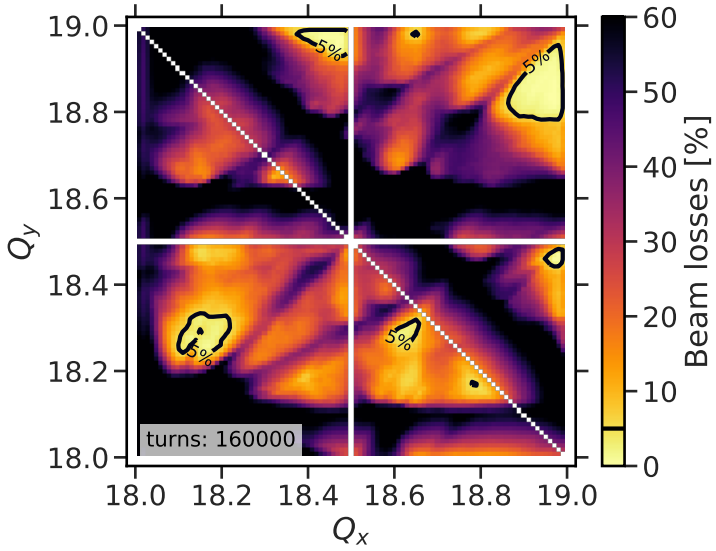

Figure: GPU simulation results for latest magnet field error model

Thanks to GSI's new high-performance GPU cluster in Green Cube:

- 400 GPU cards of today's most performant model (AMD Radeon Instinct MI100)
- even faster simulations, larger tune scans in shorter times

$\Longrightarrow$ following up magnet series production and doublet assembly

Thank you for your attention!

Acknowledgements:

GSI: O. Boine-Frankenheim, V. Chetvertkova, V. Kornilov, D. Rabusov, S. Sorge, D. Ondreka, A. Bleile, V. Maroussov, C. Roux, K. Sugita

CERN: R. de Maria, G. Iadarola, M. Schwinzerl

Grand Overview Tune Diagrams

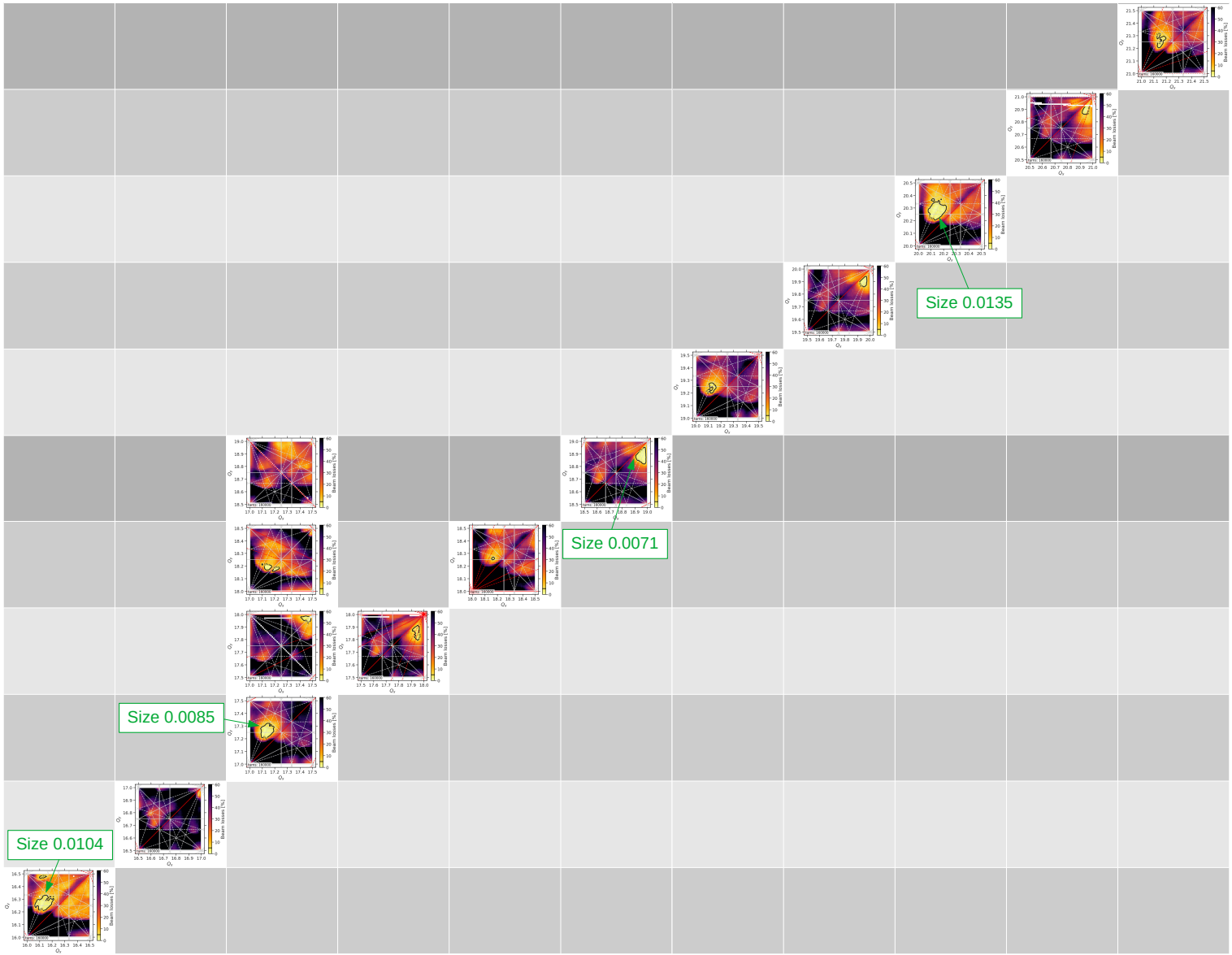

Emittance Growth at Low-loss Area

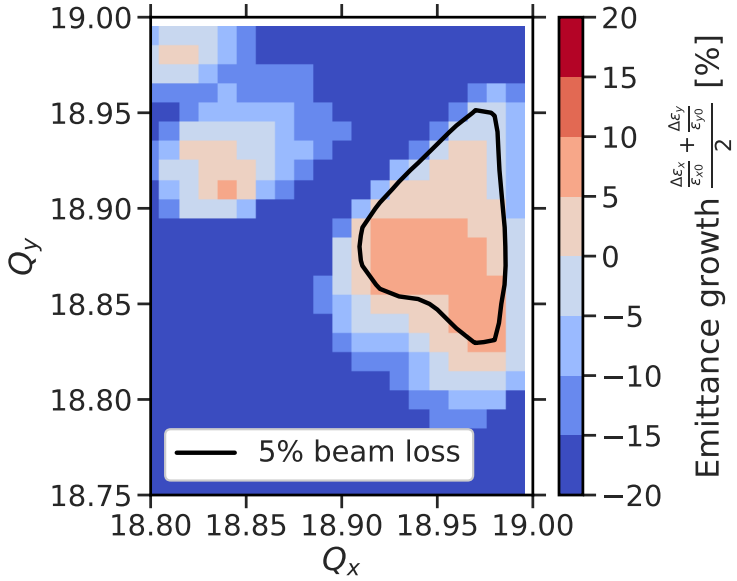

Figure: with space charge, emittance growth

PIC Results for Best Working Point

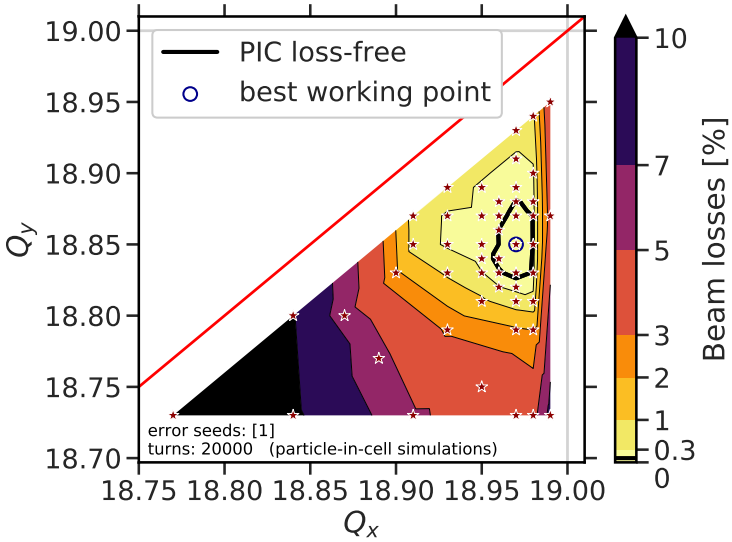

Figure: tune diagram with self-consistent PIC simulations

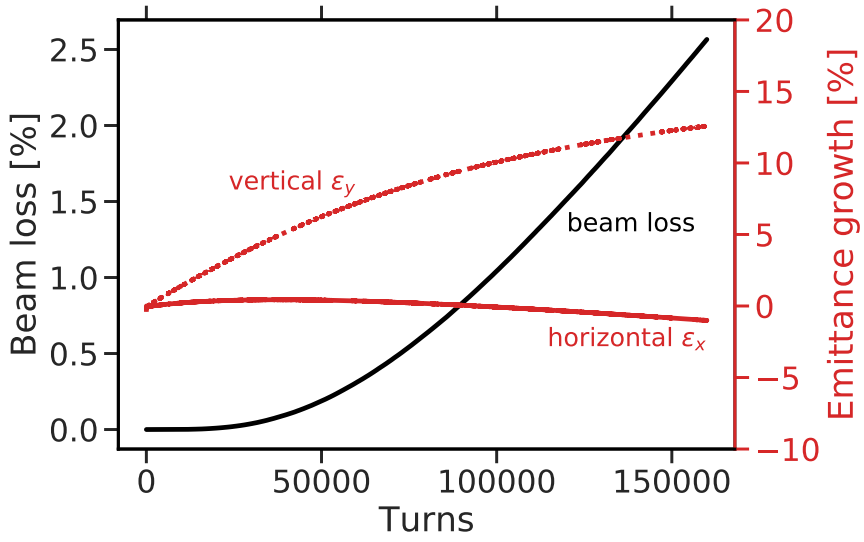

Figure: optimal working point $(Q_x, Q_y) = (18.97, 18.85)$

Comparison 2.5D to 3D PIC

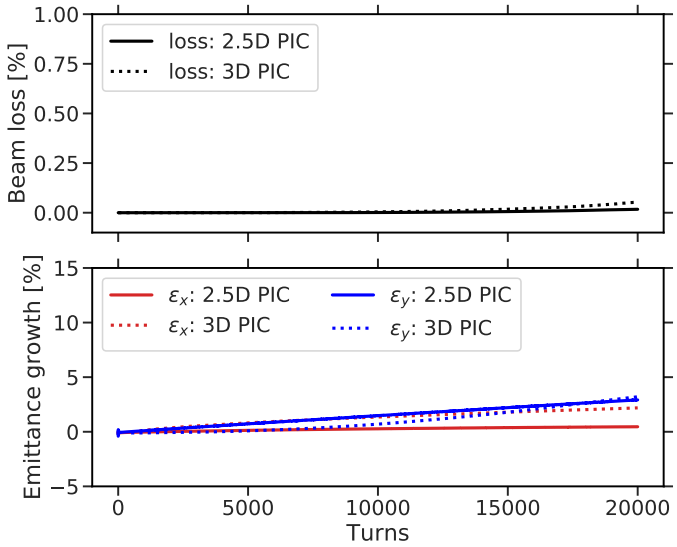

Figure: good working point $(Q_x, Q_y) = (18.97, 18.85)$

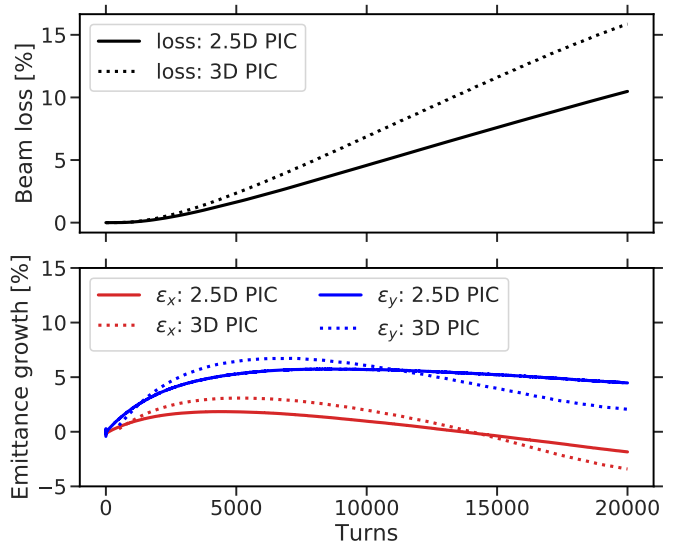

Figure: lossy working point $(Q_x, Q_y) = (18.84, 18.73)$

Adaptive Frozen SC Model